

COMPARISON OF A DISTRIBUTED BIOSPHERE HYDROLOGICAL MODEL WITH GBHM

Lei WANG¹ and Toshio KOIKE²

¹Member of JSCE, Dr. Eng., Researcher, Dept. of Civil Eng., University of Tokyo (Bunkyo-ku, Tokyo 113-8656, Japan)

²Member of JSCE, Dr. Eng., Professor, Dept. of Civil Eng., University of Tokyo (Bunkyo-ku, Tokyo 113-8656, Japan)

A distributed biosphere hydrological model, WEB-DHM was developed by embedding SiB2 into the geomorphology-based hydrological model (GBHM). Different from GBHM, WEB-DHM physically describes evapotranspiration with coupled water and energy budgets in the soil-vegetation-atmosphere transfer (SVAT) system. In this study, both WEB-DHM and GBHM have been applied to a small river basin from 2001 to 2003 with little anthropogenic effect but large interannual variability. Comparing to GBHM, WEB-DHM performs better in predictions of streamflows in terms of different time frequencies, especially in low water flow periods.

Key Words : WEB-DHM, GBHM, model comparison, streamflow, evapotranspiration

1. INTRODUCTION

In order to meet the increasing societal needs for improved hazards prediction under climate changes, distributed hydrological models (DHMs) and land surface models (LSMs) are extensively used throughout the world for better understanding the water and energy cycles.

DHMs give distributed representation of spatial variation and physical descriptions of runoff generation and routing in river channels from basin to continental scales. DHMs have been developing rapidly since the original blueprint of Freeze and Harlan¹⁾ for a physically-based distributed model. Over last thirty years, a number of DHMs incorporating new techniques appeared such as SHE²⁾ and GBHM³⁾⁴⁾. However, empirical estimation of evapotranspiration (ET) and conceptual description of land surface have been recognized as the drawbacks in traditional water-balance DHMs⁵⁾, which make it difficult for them to correctly simulate low water flows.

Meanwhile, over last several decades, LSMs have evolved from simple bucket models without vegetation consideration⁶⁾ into credible representations of water and energy fluxes in the soil-vegetation-atmosphere transfer (SVAT) systems (e.g., SiB2⁷⁾ and BATS2⁸⁾). The physical

basis of LSMs makes them an attractive alternative to the conceptual types of ET models that have traditionally been applied in hydrological modeling.

Under this circumstance, the simple biosphere model 2 (SiB2)⁷⁾ with advanced physics, and the grid-based GBHM⁴⁾ with spatially-distributed structure and physical runoff and river routing schemes, were selected to develop the distributed biosphere hydrological model incorporating subgrid topography, which is referred to as the water and energy budget-based distributed hydrological model (WEB-DHM)⁹⁾¹⁰⁾. The WEB-DHM has embedded SiB2 into the grid-based GBHM, replacing the original vertical scheme in the GBHM with a biophysical scheme to describe the SVAT system.

This study will focus on the intercomparison of WEB-DHM with GBHM⁴⁾ by using three-year (2001-2003) streamflow records with large interannual variability having high water flows in 2001 but very low water flows in 2002 and 2003. Analyses are performed in simulated streamflows in terms of different time frequencies.

2. WEB-DHM

(1) Model concept

The structure of WEB-DHM is given in **Fig.1**.

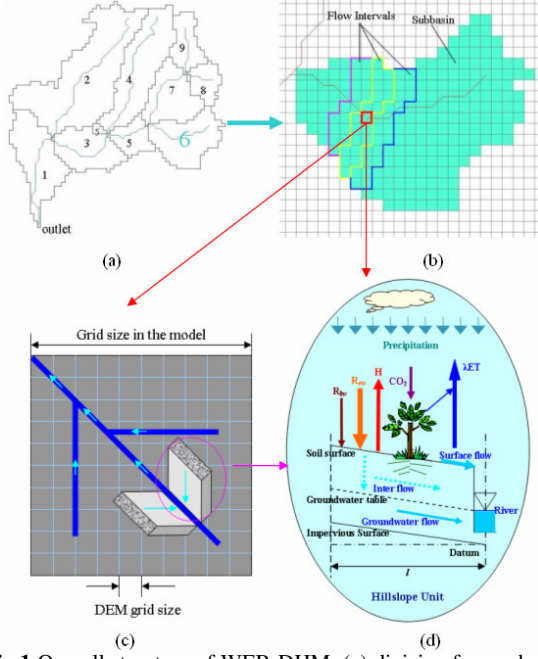


Fig.1 Overall structure of WEB-DHM: (a) division from a basin to subbasins, (b) subdivision from a subbasin to flow intervals comprising several model grids, (c) discretization from a model grid to a number of geometrically symmetrical hillslopes, and (d) process descriptions of water moisture transfer from the atmosphere to river. Here, SiB2 is used to describe the transfer of the turbulent fluxes (energy, water, and CO₂ fluxes) between the atmosphere and land surface for each model grid, where R_{sw} and R_{lw} are downward solar radiation and longwave radiation, H is the sensible heat flux, and λ is the latent heat of vaporization. GBHM simulates both surface and subsurface runoff using grid-hillslope discretization, and then simulates flow routing in the river network.

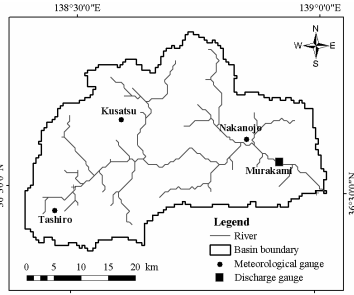


Fig.2 The Agatsuma River Basin.

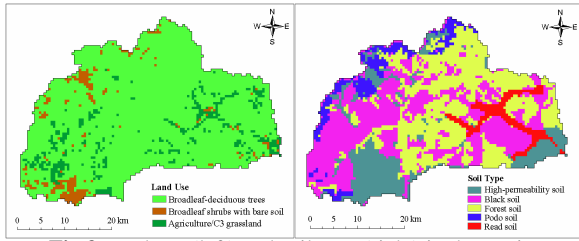


Fig.3 Land use (left) and soil type (right) in the Basin.

The model concept can be summarized as:

(i) The distributed structure of grid-based GBHM⁴⁾ has been retained to describe the catchment topography. Soil type and land use type

are assumed homogeneous in each model grid.

(ii) For each model grid in the target basin, SiB2 is used to calculate the transfer of the turbulent fluxes (energy, water, and CO₂) between atmosphere and land surface independently. Each model grid maintains its own prognostic soil moisture contents and temperatures.

(iii) In the grid-hillslope discretization constructed from the geographical information, GBHM has been used to simulate both surface and subsurface runoff generated from hillslope units and flow routing in the river network.

(2) Evapotranspiration (ET)

In WEB-DHM, the ET comes from canopy and soil surface. The ET from the canopy comprises: (i) E_{ci} evaporation from the canopy interception (comprising M_{cw} for interception water store and M_{cs} for interception snow/ice store), and (ii) E_{ct} transpiration of soil water extracted by the root system and lost from the dry fraction of canopy. Similarly, the bare soil evaporation consists of (i) E_{gi} loss from soil surface interception (comprising M_{gw} for interception water store and M_{gs} for interception snow/ice store) and (ii) E_{gs} evaporation of soil moisture from within the surface soil layer.

Details about the formulations of the ET components in WEB-DHM can be found in Sellers et al.⁷⁾, which are summarized as follows

$$\lambda E_{ct} = \left[\frac{e^*(T_c) - e_a}{1/g_c + 2r_b} \right] \frac{\rho c_p}{\gamma} (1 - W_c) \quad (1)$$

$$\lambda E_{ci} = \left[\frac{e^*(T_c) - e_a}{r_b} \right] \frac{\rho c_p}{\gamma} W_c \kappa_{T_c} \quad (2)$$

$$\lambda E_{gi} = \left[\frac{e^*(T_x) - e_a}{r_d} \right] \frac{\rho c_p}{\gamma} W_g \kappa_{T_g} \quad (3)$$

$$\lambda E_{gs} = \left[\frac{h_{soil} e^*(T_g) - e_a}{r_{soil} + r_d} \right] \frac{\rho c_p}{\gamma} (1 - W_g) \quad (4)$$

where λ is latent heat of vaporization; $e^*(T)$ is saturation vapor pressure at temperature T ; T_c is canopy temperature; T_g is soil surface temperature; $T_x = T_{snow}$ if $M_{gs} > 0$, $T_x = T_g$ if $M_{gw} > 0$; T_{snow} is the temperature of snowpack and its underlying surface soil layer; e_a is vapor pressure in canopy air space; ρ is air density; c_p is specific heat of air; γ is psychrometric constant; W_c is canopy wetness-snow cover fraction; W_g is soil wetness-snow cover fraction; $\kappa_{T_c} = 1$ when

$M_{c,gw} > 0$, $\kappa_{T_{c,g}} = \lambda/(\lambda + \lambda_s)$, when $M_{c,gs} > 0$; λ_s is heat of sublimation; g_c is canopy conductance; h_{soil} is relative humidity of the soil pore space, $h_{soil} = e^{\psi_1 g/RT_g}$ when $e^*(T_g) \geq e_a$, $h_{soil} = 1$ when $e^*(T_g) < e_a$, ψ_1 soil moisture potential of the surface layer, g acceleration due to gravity; R is gas constant; r_b is bulk canopy boundary layer resistance; r_d is aerodynamic resistance between ground and canopy air space; The soil resistance, r_{soil} , is an empirical term that is supposed to take into account the impedance of the soil pores to exchanges of water vapor between the surface soil layer and the immediately overlying air. Sun¹¹), followed by Camillo and Gurney¹²), Villalobos and Fereres¹³), and Sellers et al.¹⁴), all found it necessary to include this term to prevent the simulation of excessive soil evaporation rates. The formula for soil resistance used in WEB-DHM was derived from analyses of a large number of surface flux observations in FIFE¹⁴)

$$r_{soil} = \exp(8.206 - 4.255W_1) \quad (5)$$

where W_1 is surface soil wetness.

3. DATA

A small river basin (Agatsuma; see Fig.2) with fine observations was selected to compare the performance between GBHM and WEB-DHM.

The Agatsuma River Basin, a sub-basin of the upper Tone River Basin, is located northwest to Tokyo. The elevation of this basin varies from about 200 m to 2500 m. The catchment area lying upstream of the Murakami gauge is about 1,300 km². Only a very small reservoir was completed in the upstream and thereby not considered in this study.

The DEM and land use were obtained from the Japan Geographical Survey Institute. Subgrid topography is described by a 50 m resolution DEM. Land use data was reclassified to 3 SiB2 categories (Fig.3; left), with broadleaf-deciduous tree as a dominant type. The type-dependent vegetation static parameters comprising morphological properties, optical properties and physiological properties are defined following Sellers et al.¹⁵). The dynamic vegetation parameters are Leaf Area Index (LAI), and the Fraction of Photosynthetically Active Radiation absorbed by the green vegetation canopy (FPAR), which can be obtained from satellite data. Global LAI and FPAR MOD15_BU 1 km data sets¹⁶) were used in this study, which are 8-daily composites of MOD15A2 products and were provided from EOS Data Gateway of NASA. Soil

type (Fig.3; right) was processed from a 1:200,000 scale Gunma Prefecture geological map. This paper set related soil static parameters following a previous study in the upper Tone River Basin⁴).

The hourly precipitation data were obtained from the Radar-AMeDAS (Automated Meteorological Data Acquisition System) rainfall analysis data, which combines both radar and ground observations, provided by the Japanese Meteorological Agency (JMA). The data are available at 5 km spatial resolution until March of 2001 and 2.5 km spatial resolution later. The surface meteorological data other than precipitation includes air temperature, relative humidity, and air pressure, wind speed, as well as downward solar and longwave radiation. Air temperature, wind speed, and sunshine duration were from AMeDAS annual report of JMA. The downward solar radiation was estimated from sunshine duration, temperature, and humidity, using a hybrid model developed by Yang et al.¹⁷⁾¹⁸). The longwave radiation was then estimated from temperature, relative humidity, pressure, and solar radiation using the relationship between solar radiation and longwave radiation¹⁹). All the inputs were interpolated to a 500 m grid for model simulations.

4. RESULTS AND DISCUSSIONS

Both GBHM and WEB-DHM were fed with the same forcing data, soil and vegetation parameters including LAI. For GBHM, potential ET (E_p) was estimated with the same meteorological data using the Priestley-Taylor's method²⁰)

$$E_p = \alpha \frac{s}{s + \gamma} (R_n - G) \quad (6)$$

where α is set to 1.26 for the basin (humid climate); s is the slope of the saturation specific humidity-temperature curve at air temperature; R_n is the net radiation, and G is the soil heat flux. ET estimation by GBHM can be found in Appendix A.

Surface layer was defined as 0.05 m, and top soil depth 2 m with the type-dependent root depth defined by Sellers et al.¹⁵). Initial soil and groundwater conditions were obtained by running WEB-DHM with the forcing data of year 2000. Simulations were performed from 2001 to 2003 with the same initial conditions by using GBHM and WEB-DHM in hourly time step and 500 m spatial resolution.

(1) Evaluation criterion

Both Nash-Sutcliffe model efficiency coefficient (NS)²¹) and Bias Error ($BIAS$) are used to evaluate the models' performance. The NS is defined as

$$NS = 1 - \frac{\sum_{i=1}^n (Q_{oi} - Q_{si})^2}{\sum_{i=1}^n (Q_{oi} - \overline{Q_o})^2} \quad (7)$$

Where, Q_{oi} is observed discharge; Q_{si} is simulated discharge; n is the total number of time series; $\overline{Q_o}$ is the mean observed discharge over the simulation period. The *BIAS* is defined as

$$BIAS = \frac{\sum_{i=1}^n (Q_{si} - Q_{oi})}{\sum_{i=1}^n Q_{oi}} \quad (8)$$

(2) Results and discussions

Table 1 showed the annual water budget simulated by the two models. WEB-DHM represented the interannual variation much better than GBHM, with smaller *BIAS* in simulated runoff for most years, although the three-year total runoff was well estimated by both of them.

Fig.4 gave the monthly discharge at Murakami from 2001 to 2003. In 2001, GBHM showed comparable performance to WEB-DHM. But in 2002 and 2003 with annual runoff less than 50% of that in year 2001, WEB-DHM with *NS* equal to 0.768 performed much better than GBHM with *NS*

Table 1 Comparison of annual water budgets from 2001 to 2003 simulated by GBHM and WEB-DHM.

Model	Year	Prep. (mm)	ET (mm)	Runoff		
				R_{sim} (mm)	R_{obs} (mm)	BIAS (%)
GBHM	2001	1285	570	787	818	-4
	2002	1083	577	514	408	26
	2003	962	537	353	404	-13
	Total	3329	1684	1655	1630	1.54
WEB-DHM	2001	1285	580	759	818	-7
	2002	1083	589	485	408	19
	2003	962	511	409	404	1
	Total	3329	1681	1654	1630	1.48

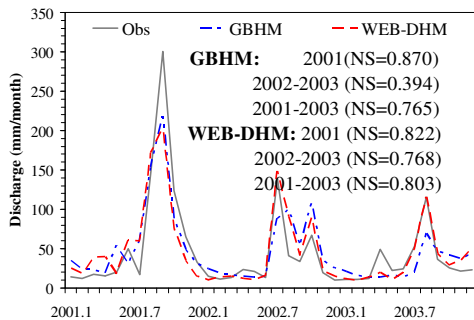


Fig.4 Simulated and observed monthly discharge at Murakami from 2001 to 2003.

equal to 0.394. For daily discharges given in **Fig.5**, WEB-DHM also got a higher *NS* (0.829) than that of GBHM (0.789). The logarithmic daily hydrographs clearly showed that WEB-DHM reproduced the streamflows in low flow periods (2002-2003) much better than GBHM. The scatterplots in **Fig.6** confirmed the better performance of WEB-DHM.

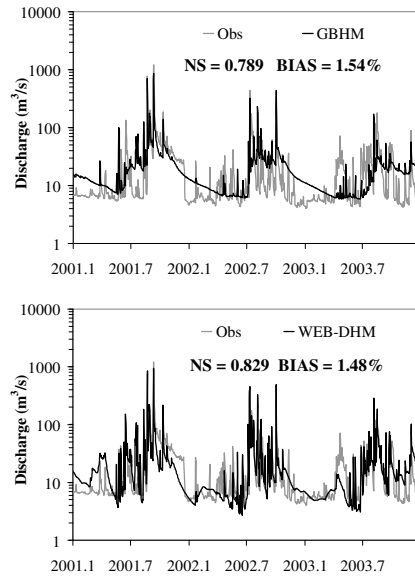


Fig.5 Logarithmic daily hydrographs at Murakami from 2001 to 2003 simulated with GBHM (upper) and WEB-DHM (lower).

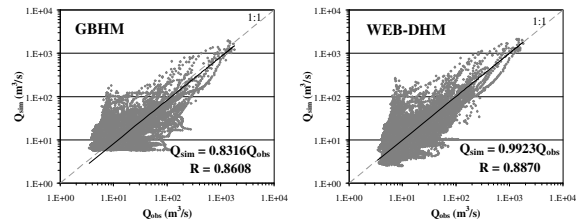


Fig.6 Scatterplots of hourly discharges at Murakami from 2001 to 2003 simulated with GBHM (left) and WEB-DHM (right). In each plot, the best fit line (solid) and a 1:1 line (dotted) are included for comparison.

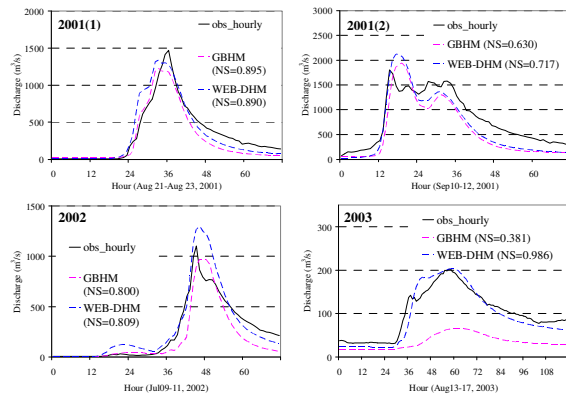


Fig.7 Observed and simulated hourly annual largest flood peaks at Murakami from 2001 to 2003 with GBHM and WEB-DHM.

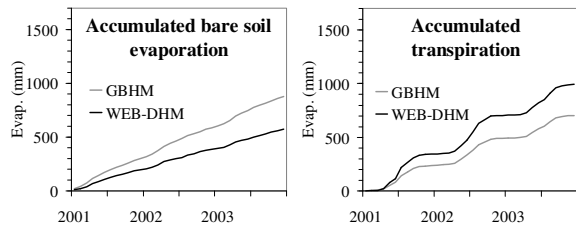


Fig.8 Accumulated bare soil evaporation (left) and transpiration (right) averaged at the upper area of Murakami.

The simulated hourly annual largest flood peaks during the long-term continuous simulation from 2001 to 2003 were compared with hourly ground observations in **Fig.7**. In 2001, there were two continuous large flood peaks with the former occurring 21-23 August and the latter 10-12 September. Generally, hourly annual largest flood peaks at Murakami were well reproduced by WEB-DHM with most *NS* greater than 0.8 (see **Fig.7**). In most cases, the differences between simulated and observed annual largest flood peaks were less than 20%. The flood peak time were well reproduced with most of the time differences less than 2 hours. For GBHM, the simulated hourly annual largest flood peaks agreed well with observations in 2001 and 2002, but had large discrepancy in the flood peak of 2003. Consequently, GBHM got a much lower *NS* (0.381) than that from WEB-DHM (0.986).

The underestimations of flood peaks were possibly attributed to the different ET schemes used in GBHM and WEB-DHM. Although the ET estimated by the two models appeared very similar in terms of total amount (**Table 1**), bare soil evaporations and transpirations simulated by them were very different. In this study, the simulated bare soil evaporation from WEB-DHM was consistently lower than the result from GBHM (**Fig.8**; left), with 35% lower with respect to the total bare soil evaporation. This is mainly because that WEB-DHM incorporating SiB2 specifies a soil resistance term to take into account the impedance of the soil pores to exchanges of water vapor between the surface soil layer and the immediately overlying air, while GBHM does not²²⁾.

As a result, GBHM obtained a much lower transpiration than WEB-DHM (**Fig.8**; right), due to the water budget constraint. The different ET estimations by the two models thus contributed to the different simulated discharges by them at Murakami from 2001 to 2003. The lower transpiration from the root zone simulated by GBHM resulted in the overestimation of the subsurface runoff (see **Fig.5**). On the other hand, the excessive bare soil evaporation calculated by GBHM caused more infiltration and thus the underestimation of the surface runoff (see **Fig.7**). Of course, it is possible to increase the transpiration

rate of GBHM to reduce the subsurface runoff through tuning the crop coefficient (K_c ; see Appendix A). However, that will result in the overestimation of the total ET by GBHM, corrupting the simulation of water budget.

5. CONCLUDING REMARKS

In this study, GBHM and WEB-DHM were compared in the Agatsuma River Basin using three-year (2001-2003) streamflow records at the Murakami gauge, which has a large interannual variability. Results showed that the new coupled model (WEB-DHM) incorporating SiB2 generally gave better performance than GBHM in predictions of the streamflows with different time frequencies, especially in low water flow periods (2002 and 2003).

This study has shown the improvements of WEB-DHM over GBHM, a traditional water balance model. Generally speaking, in a basin-scale hydrological simulation, ET plays an important role in determining both long-term water budgets and short-term flood events. First, ET determines the partition from precipitation to runoff and ET from monthly to longer timescales. Second, the accurate estimation of ET in an earlier simulation is crucial to obtain initial soil moisture conditions for flood event simulation, especially in low water flow conditions. Therefore, to improve both water budget studies and flood predictions for a region, it is important that the energy budget be investigated to improve our understanding of the water and energy cycles that are coupled in a basin.

Meanwhile, the introduction of SiB2 to simulate the land-atmosphere interactions increases the model complexity and computation cost. In this study, the computation time for one-year simulation of the Agatsuma River Basin (5399 model grids) in Red Hat Linux release 8.0 workstation (CPU: 3.0 GHz) were 0.2 h and 0.75 h spent by GBHM and WEB-DHM, respectively. Further efforts including the adoption of parallel computing²³⁾ are expected to improve the efficiency of WEB-DHM.

From the view of hydrological applications, GBHM and WEB-DHM can contribute to different purposes. GBHM is suitable for hydrological simulations in relatively high-flow conditions; while WEB-DHM can be used for the investigation of water and energy cycles of a basin in both high- and low-flow conditions.

ACKNOWLEDGMENT: This study was funded by Core Research for Evolutional Science and Technology, the Japan Science and Technology Corporation. Parts of this work were also supported by grants from the Ministry of Education, Culture,

Sports, Science and Technology of Japan, and Japan Aerospace Exploration Agency. Global 8-daily MODIS Terra LAI/FPAR 1 km data sets are from the EOS Data Gateway of NASA. We thank three anonymous reviewers whose comments helped improve the paper.

APPENDIX A ET Estimation by GBHM

In GBHM, the four ET components are estimated as follows³⁾²²⁾

$$E_{ct} = [K_v K_c E_p] f_1(z) f_2(\theta) \frac{LAI}{LAI_0} \quad (A1)$$

$$E_{ci} = \begin{cases} K_v K_c E_p, & M_c \geq K_v K_c E_p \Delta t \\ M_c / \Delta t, & M_c < K_v K_c E_p \Delta t \end{cases} \quad (A2)$$

$$E_{gi} = \begin{cases} E_p(1 - K_v), & M_g \geq E_p(1 - K_v)\Delta t \\ M_g / \Delta t, & M_g < E_p(1 - K_v)\Delta t \end{cases} \quad (A3)$$

$$E_{gs} = [E_p(1 - K_v) - E_{gi}] f_2(\theta) \quad (A4)$$

where K_v is the vegetation coverage; K_c is the crop coefficient; $f_1(z)$ is the root distribution function which is treated as linear function, and z is the average depth of this layer; $f_2(\theta)$ is soil moisture function which is treated as linear decreasing from field capacity to wilting point, and θ is the soil moisture content; LAI is the leaf-area-index; LAI_0 is the maximum leaf-area-index of the vegetation in a year; Δt is time interval; M_c is the canopy interception; M_g is the soil surface interception.

REFERENCES

- 1) Freeze, R. A. and Harlan, R. L. : Blueprint for a physically-based digitally-simulated hydrological response model, *J. Hydrol.*, Vol. 9, pp. 237-258, 1969.
- 2) Abbott, M. B., Bathurst, J. C., Cunge, J. A., O'Connell, P. E. and Rasmussen, J. : An introduction to the European hydrological system-Systeme Hydrologique Europeen, SHE, 2. Structure of a physically-based distributed modeling system, *J. Hydrol.*, Vol. 87, pp. 61-77, 1986.
- 3) Yang, D. : Distributed hydrological model using hillslope discretization based on catchment area function: development and applications, *Ph.D. thesis*, Univ. of Tokyo, Tokyo, 1998.
- 4) Yang, D., Koike, T., and Tanizawa, H. : Application of a distributed hydrological model and weather radar observations for flood management in the upper Tone River of Japan, *Hydrol. Process.*, Vol. 18, 3119-3132, 2004.
- 5) Tang, Q., Oki, T. and Kanae, S. : A distributed biosphere hydrological model (DBHM) for large river basin, *Ann. J. Hydraul. Eng.-JSCE*, Vol. 50, pp. 37-42, 2006.
- 6) Manabe, S. : Climate and ocean circulation. I. Atmospheric circulation and circulation and hydrology of earth's surface, *Mon. Weather Rev.*, Vol. 97, pp. 739-774, 1969.
- 7) Sellers, P. J., Randall, D. A., Collatz, G. J., Berry, J. A., Field, C. B., Dazlich, D. A., Zhang, C., Collelo, G. D. and Bounoua, L. : A revised land surface parameterization (SiB2) for atmospheric GCMs. 1. Model formulation, *J. Climate*, Vol. 9, pp. 676-705, 1996.
- 8) Dickinson, R. E., Shaikh, M., Bryant, R. and Graumlich, L. : Interactive canopies for a climate model, *J. Climate*, Vol. 11, pp. 2823-2836, 1998.
- 9) Wang, L. : Development of a distributed runoff model coupled with a Land Surface Scheme, *Ph.D. thesis*, University of Tokyo, Tokyo, 2007.
- 10) Wang, L., Koike, T., Yang, K., Jackson, T., Bindlish, R. and Yang, D. : Development of a distributed biosphere hydrological model and its evaluation with the Southern Great Plains Experiments (SGP97 and SGP99), *J. Geophys. Res.-Atmos.*, Accepted, 2008.
- 11) Sun, S.: Moisture and heat transport in a soil layer forced by atmospheric conditions, *M.S. thesis*, Dept. of Civil Engineering, University of Connecticut, pp. 72, 1982.
- 12) Camillo, P. and Gurney, R. J.: A resistance parameter for bare soil evaporation models, *Soil Sci.*, Vol. 141, pp. 94-105, 1986.
- 13) Villalobos, F. J. and Fereres, E.: Evaporation measurements beneath corn, cotton and sunflower canopies, *Agron. J.*, Vol. 82, pp. 1153-1159, 1990.
- 14) Sellers, P. J., Heiser, M. D. and Hall, F. G.: Relationship between surface conductance and spectral vegetation indices at intermediate (100 m² - 15 m²) length scales, *J. Geophys. Res. FIFE Special Issue*, Vol. 97, pp. 19033-19060, 1992.
- 15) Sellers, P. J., Los, S. O., Tucker, C. J., Justice, C. O., Dazlich, D. A., Collatz, G. J. and Randall, D. A. : A revised land surface parameterization (SiB2) for atmospheric GCMs, Part II: The generation of global fields of terrestrial biophysical parameters from satellite data, *J. Climate*, Vol. 9, pp. 706-737, 1996.
- 16) Myneni, R. B., Nemani, R. R. and Running, S. W. : Algorithm for the estimation of global land cover, LAI and FPAR based on radiative transfer models, *IEEE. T. Geosci. Remote*, Vol. 35, pp. 1380-1393, 1997.
- 17) Yang, K., Huang, G. and Tamai, N. : A hybrid model for estimating global solar radiation, *Sol. Energy*, Vol. 70, pp. 13-22, 2001.
- 18) Yang, K., Koike, T. and Ye, B. : Improving estimation of hourly, daily, and monthly solar radiation by importing global data sets. *Agr. Forest Meteorol.*, Vol. 137, pp. 43-55, 2006.
- 19) Crawford, T. M. and Duchon, C. E. : An improved parameterization for estimating effective atmospheric emissivity for use in calculating daytime downwelling longwave radiation, *J. Appl. Met.*, Vol. 38, pp. 474-480, 1999.
- 20) Priestley, C. H. B. and Taylor, R. J. : On the assessment of surface heat flux and evaporation using large-scale parameters, *Mon. Weather Rev.*, Vol. 100, pp. 81-92, 1972.
- 21) Nash, J. E. and Sutcliffe, J. V. : River flow forecasting through conceptual models part I - A discussion of principles. *J. Hydrol.*, Vol. 10, pp. 282-290, 1970.
- 22) Yang, D., Herath, S. and Musiak, K. : Comparison of different distributed hydrological models for characterization of catchment spatial variability, *Hydro. Process.*, Vol. 14, pp. 403-416, 2000.
- 23) Almasi, G. S. and Gottlieb, A. : *Highly Parallel Computing*, Benjamin-Cummings publishers, Redwood City, CA, 1989.

(Received September 30, 2008)